

Non-Gaussian statistics of electrostatic fluctuations of hydration shells

Allan D. Friesen¹ and Dmitry V. Matyushov^{1, a)}

Center for Biological Physics, Arizona State University, PO Box 871604, Tempe, AZ 85287-1604

We report the statistics of electric field fluctuations produced by SPC/E water inside a Kihara solute given as a hard-sphere core with a Lennard-Jones layer at its surface. The statistics of electric field fluctuations, obtained from numerical simulations, are studied as a function of the magnitude of a point dipole placed close to the solute-water interface. The free energy surface as a function of the electric field projected on the dipole direction shows a cross-over with the increasing dipole magnitude. While it is a single-well harmonic function at low dipole values, it becomes a double-well surface at intermediate dipole moment magnitudes, transforming to a single-well surface, with a non-zero minimum position, at still higher dipoles. A broad intermediate region where the interfacial waters fluctuate between the two minima is characterized by intense field fluctuations, with non-Gaussian statistics and the variance far exceeding the linear-response expectations. The excited state of the surface water is found to be lifted above the ground state by the energy required to break approximately two hydrogen bonds. This state is pulled down in energy by the external electric field of the solute dipole, making it readily accessible to thermal excitations. The excited state is a localized surface defect in the hydrogen-bond network creating a stress in the nearby network, but otherwise relatively localized in the region closest to the solute dipole.

Keywords: Hydration, surface phase transition, hydrogen bonds, optical spectroscopy, solvent effect

I. INTRODUCTION

Polarization of polar liquids by external electric fields is one of classical problems of condensed matter theory.^{1,2} The ideas advanced by Debye and Langevine assign the average dipole moment in a liquid exposed to an external electric field to a function increasing monotonically and linearly (Debye) or non-linearly, with saturation (Langevine) with the increasing field strength.³ The polarized medium, in return, produces a field of its own which, combined with the external field, yields the macroscopic Maxwell field. One thus arrives at the concept of dielectric screening implying the ability, quantified by the macroscopic dielectric constant, of the medium to polarize and produce its own electric field, in response to an external perturbation.

The electric field of a polar liquid can be alternatively probed by an external multipole. The electric field $\mathbf{R}(\Gamma)$ inside a liquid is a fluctuating variable depending on the instantaneous liquid configuration represented by a point in its phase space Γ . Thus an external dipole moment \mathbf{m}_0 placed outside or inside the liquid will gain the instantaneous electric energy $e = -\mathbf{m}_0 \cdot \mathbf{R}$. The liquid, in turn, is polarized by \mathbf{m}_0 such that its field at the position of the dipole fluctuates around the average field \mathbf{R}_0 , which is aligned along \mathbf{m}_0 and is known as the Onsager reaction field.⁴ This average field is accessible experimentally from solvent-induced shifts of optical dyes.^{5,6}

A fluctuation of the electric field $\delta\mathbf{R}(\Gamma) = \mathbf{R}(\Gamma) - \mathbf{R}_0$ out of equilibrium requires reversible, non-expansion work applied to the system;⁷ this work is quantified by the Landau functional $F(\mathbf{R})$. We will be interested here

only in the projection of the field on the direction $\hat{\mathbf{m}}_0 = \mathbf{m}_0/m_0$ of the external dipole and thus will set up the “reaction coordinate” or “order parameter” $R = \hat{\mathbf{m}}_0 \cdot \mathbf{R}$.⁷ The free energy surface can then be found by standard prescriptions⁸ singling out the order parameter from the manifold of the system degrees of freedom

$$e^{-\beta F(R)} \propto \int \delta(R - R(\Gamma)) e^{-\beta H} d\Gamma. \quad (1)$$

In this equation, H is the Hamiltonian of the solution involving a solute carrying no dipole ($\mathbf{m}_0 = 0$), and $\beta = 1/(k_B T)$ is the inverse temperature. The free energy $F(R)$ thus describes thermal fluctuations of the electric field in the absence of the dipole \mathbf{m}_0 .

Empirical observations suggest that the Onsager reaction field R_0 is a linear function of the dipole moment inducing it.^{5,6} This observation can be mathematically cast into the requirement of a harmonic form of $F(R)$ (Fig. 1a)

$$F(R) = R^2/(2\kappa). \quad (2)$$

The free energy changes when the dipole moment is turned on into

$$\mathcal{F}(m_0, R) = -m_0 R + F(R). \quad (3)$$

The minimization of this free energy in respect to the field R yields the reaction field linear in the solute dipole, $R_0 = \kappa m_0$. This is the familiar linear response approximation.⁹ It articulates two physically significant concepts: (i) the response of the medium (here electric field) grows linearly with an external perturbation (solute dipole moment) and (ii) the perturbation does not alter the spectrum of the medium fluctuations which therefore can be calculated or measured from the properties of the

^{a)}Electronic mail: dmitrym@asu.edu

system in the absence of the perturbation (zero-dipole solute in our case).

The distribution of the solvent electric field $P(R) \propto \exp[-\beta F(R)]$ is a Gaussian function with the variance $\sigma_R^2 = \langle (\delta R)^2 \rangle$ equal to κ/β , $\delta R = R - R_0$. Since fluctuations of the electric field introduce fluctuations in the optical transition energies,^{10–13} the stiffness parameter κ (also known as response function) is experimentally accessible from the inhomogeneous width of an optical line. At the same time, since the average energy, $e_0 = -\kappa m_0^2$, and the distribution width are given in terms of the same parameter κ , one gets the fluctuation-dissipation⁹ relation between the average energy and the energy variance, $e_0 = -\beta \langle (\delta e)^2 \rangle$. The parameter

$$\chi_G = -\beta \langle (\delta e)^2 \rangle / e_0 \quad (4)$$

can therefore be considered as the non-linearity parameter quantifying deviations from the Gaussian statistics of the electric field fluctuations.¹⁴ $\chi_G = 1$ for the Gaussian statistics when linear response holds and the stiffness parameter can be calculated either from the reaction field or from the field variance

$$\kappa = R_0/m_0 = \beta \sigma_R^2. \quad (5)$$

The inverse stiffness parameter κ^{-1} has the meaning of the characteristic volume in which a small probe dipole will be influenced by the fluctuations of the electric field R . One can then introduce the characteristic length to which the field fluctuations penetrate inside the solute

$$\ell_R = (\kappa)^{-1/3} \quad (6)$$

This length will then define the thickness of the surface layer within which a dipolar probe (e.g., optical dye) will be affected by the solvent (i.e., the interaction energy will be greater than $k_B T$).

The harmonic free energy profile [Eq. (2)] sketched in Fig. 1a is not the only conceivable form of the free energy surface. The reaction field R_0 building up in response to a growing dipole moment m_0 is produced by the solvent dipoles increasingly aligned with the external field. This externally forced alignment leads to frustration of the local orientational structure within the liquid, which can release itself into a new structure represented by a second minimum of the Landau functional $F(R)$ (Fig. 1b).

Several fundamental consequences might be anticipated if the situation sketched in Fig. 1b is realized. First, the curvature of the free energy at the higher-energy minimum is not necessarily equal to the curvature at the lower-energy minimum. In other words, the fluctuation spectrum around the minimum R_1 might be altered compared to the spectrum in the absence of the external field. If this happens, the assumption (ii) listed above (no alteration to the fluctuation spectrum) does not apply anymore. Further, the free energy F_0 at the second minimum should be lifted compared to $F(0) = 0$ in expectation of no spontaneous field in the ground state. However, the field of the dipole m_0 will bring the minimum

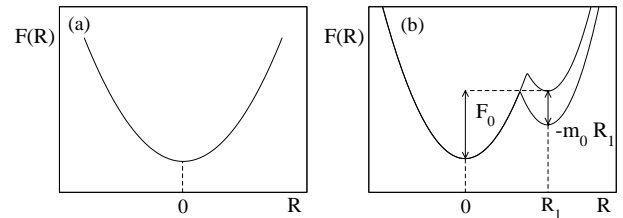


FIG. 1. Sketch of the standard expectation (a) and the picture proposed in this study (b) for the free energy of creating field R at a point within the solute when no dipole is present [Eq. (1)]. In our simulations, a point dipole is placed at that point, which modifies the free energy to $\mathcal{F}(m_0, R)$ [Eq. (3)]. The traditional linear-response approximation anticipates $F(R)$ to be harmonic in the whole range of R -values of interest. In contrast, we suggest the existence of an excitation state, with the corresponding minimum lifted by the free energy F_0 . This excited state, too high to be observed in the homogeneous liquid or in non-polar solution, can become observable by placing the dipole m_0 into the solute, which lowers the free energy gap between the lower and higher minima by $-m_0 R_1$. The curvature of the excited state near its minimum might be different from the corresponding curvature at the lower minimum, thus altering the basic assumption of the linear-response approximation, the invariance of the spectrum of the solvent fluctuations with respect to the magnitude of m_0 . The overall shift of $F(R)$ in the external field is not shown in the diagram; the positions of the lower minimum at zero and nonzero dipoles m_0 are therefore made coincide.

of $\mathcal{F}(m_0, R)$ down by $-m_0 R_1$ (Fig. 1). This external-field effect offers a unique opportunity to study excitation states of a liquid interface not significantly populated by thermal excitations due to a high value of F_0 .

Interfaces of water with solutes of nanometer dimension is a particularly suitable candidate for observing surface excited states. Large solutes break the network of hydrogen bonds of bulk water producing unsatisfied surface bonds. The result is a specific orientational structure of the surface waters with their dipoles preferentially oriented parallel to the interface.^{15–17} While strong hydrogen-bond interactions provide a sufficient driving force for in-plane orientations, the electric field of external multipoles will compete with this alignment, possibly switching it, in a discontinuous fashion, into a new interfacial structure. In fact, Sharp and co-workers have found that water at the solute interface occupies two states of local structure characterized by straight, “ice-like” hydrogen bonds around non-polar solutes and bent bonds, required by the dipoles alignment along the electrostatic field of polar/ionic solutes.^{18,19} The distinction between polar and non-polar solvation can be attributed in this picture to changes in occupations of these two hydrogen bonding states. What has been still missing from that picture is the ability of surface waters to switch between the two states via a concerted cross-over. The existence of such a cross-over, occurring with increasing electrostatic field of the solute, is the main finding of this study.

The system we study here is a non-polar solute im-

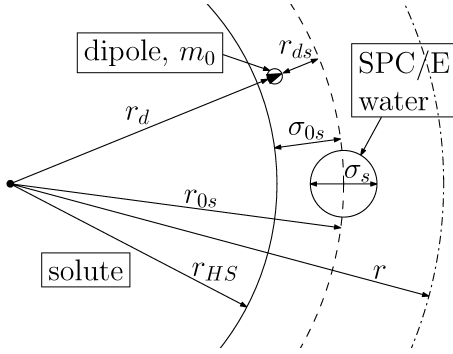


FIG. 2. Cartoon of the solute-solvent configuration. The solute is a hard core of radius r_{HS} covered with the LJ layer of the width σ_{0s} [Eq. (7)]. The distance $r_{0s} = r_{HS} + \sigma_{0s}$ approximately corresponds to the first peak of the solute-solvent pair distribution function $g_{0s}(r)$ [also see Fig. 8 below]. The point dipole m_0 is placed at the distance r_d from the solute center and, correspondingly, the distance $r_{ds} = r_{0s} - r_{HS}$ from the solute-solvent interface. The solvent is SPC/E water at 1 atm and 273 K (the melting temperature of SPC/E water is 215 K²⁰).

mersed in SPC/E water²⁰ and interacting with it by a Kihara potential characterized by a hard-sphere core, $r_{HS} = 9 \text{ \AA}$, and two Lennard-Jones (LJ) parameters, $\sigma_{0s} = 3 \text{ \AA}$ and $\epsilon_{0s} = 0.65 \text{ kJ/mol}$,

$$\phi_{0s}(r) = 4\epsilon_{0s} \left[\left(\frac{\sigma_{0s}}{r - r_{HS}} \right)^{12} - \left(\frac{\sigma_{0s}}{r - r_{HS}} \right)^6 \right]. \quad (7)$$

We then modify the system by introducing a dipole moment at the distance r_d from the solute center (Fig. 2) and watch the changes in the distribution of the water field R experienced by the dipole when the dipole magnitude grows. While the system follows the standard expectations of linear response at low solute dipoles m_0 , the situation changes at some critical value of the solute dipole when a new, non-linear, functional form for the reaction field emerges (Fig. 3). The reaction field returns to a linear trend with m_0 when the dipole keeps growing, but extrapolates to a non-zero value at $m_0 \rightarrow 0$, as would be expected if the system has landed in a high free-energy minimum, as in Fig. 1b. Further, the curvature around this second minimum (slope of R_0 vs m_0 in Fig. 3) also experiences alteration, as we have described above. The basic physical picture is the emergence of a finite domain of surface waters in an excited state different both from the bulk and from the rest of the interface. The details of the simulation protocol can be found in the Supplementary Material (SM)²¹ and we proceed to the discussion of the results.

II. THREE-STATE MODEL

Before proceeding to a more detailed description of the simulation results, we briefly outline the analytical frame-

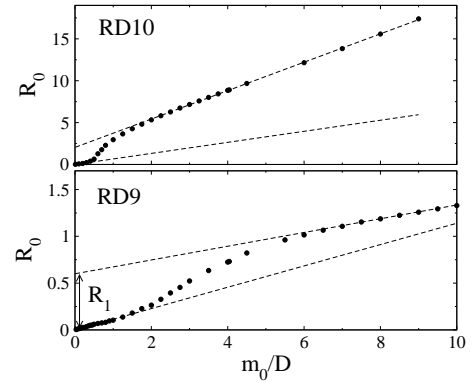


FIG. 3. Reaction field R_0 (in V/Å) vs solute dipole m_0 for RD9 ($r_d = 9 \text{ \AA}$) and RD10 ($r_d = 10 \text{ \AA}$) configurations (see Fig. 2). The dashed lines show the slopes of the linear portions of $R_0(m_0)$. The scaling of R_0 with m_0 is approximately quadratic in the intermediate region. The vertical arrow in the lower panel indicates the equilibrium field R_1 in the excited state obtained by extrapolating the reaction field in the excited configuration to zero solute dipole (Fig. 1).

work used here to understand the outcome of the simulations. This is a phenomenological three-state model representing the simulation data in terms of three distinct states of surface waters.

The model includes three states described by Landau free energy functions $F_\alpha(R)$ [Eq. (1)] with $\alpha = g, 1, 2$ standing for the ground state (g) and two excited states corresponding to the minima R_α at the positive (1) and negative (2) reaction field values. Two excited states, instead of one as in Fig. 1, are introduced to satisfy the condition of vanishing reaction field at $m_0 \rightarrow 0$. The minima of these states are lifted by the energies F_α from the free energy minimum $F_g(0)$ of the ground state. Each of $F_\alpha(R)$ curves is modified by the presence of an external dipole m_0 into $\mathcal{F}_\alpha(m_0, R) = F_\alpha(R) - m_0 R$, as in Eq. (3). The global free energy of the system is then found as the statistical trace over the three states as follows

$$e^{-\beta\mathcal{F}(m_0, R)} = \sum_{\alpha} e^{-\beta\mathcal{F}_\alpha(m_0, R)}. \quad (8)$$

From MD simulations, we have found little asymmetry in the distribution of water's dipolar directions at the interface, as judged from the first-order orientational parameter

$$p_1^I = (N^I)^{-1} \sum_{j=1, N^I} \hat{\mathbf{m}}_j \cdot \hat{\mathbf{r}}_j. \quad (9)$$

Here, the sum runs over N^I waters in the solute's first hydration layer, $\hat{\mathbf{m}}_j = \mathbf{m}_j/m$, and $\hat{\mathbf{r}}_j = \mathbf{r}_j/r_j$ is the unit vector defining the position of the first-shell water relative to the solute's center. The order parameter p_1^I is close to zero indicating that dipoles oriented parallel and antiparallel to the surface normal occur with approximately equal probability. Therefore, the average field at

$$m_0 = 0$$

$$\langle \mathbf{R} \rangle = \sum_j \mathbf{T}(\mathbf{r}_d - \mathbf{r}_j) \cdot \langle \mathbf{m}_j \rangle, \quad (10)$$

(\mathbf{T} is the dipolar tensor) is expected to approach zero.

One needs to mention that the orientational structure of surface water around spherical cavities and non-polar solutes results in a positive value of the cavity electrostatic potential.^{12,22} The potential is apparently rather uniform resulting in $\langle \mathbf{R} \rangle \simeq 0$ in both the present simulations with the off-center dipole, as well as in our previous study of the same Kihara solute with the dipole placed at the solute's center.²³

In contrast to the first-order orientational order parameter p_1^I the second-order orientational parameter

$$p_2^I = (2N^I)^{-1} \sum_{j=1, N^I} [3(\hat{\mathbf{m}}_j \cdot \hat{\mathbf{r}}_j)^2 - 1] \quad (11)$$

is of the order $p_2^I \simeq -0.19$, indicating that about 40% of first-shell waters have their dipoles directed perpendicular to the surface normal.¹⁵⁻¹⁷ This parameter decays only slightly upon the insertion of the solute dipole (Fig. 4).

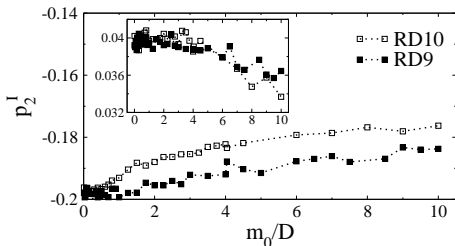


FIG. 4. Second [p_2^I , Eq. (11)] (main panel) and first [p_1^I , Eq. (9)] (inset) orientational order parameters for RD9 ($r_d = 9$ Å, filled squares) and RD10 ($r_d = 10$ Å, open squares) configurations.

Taken together, the results for $p_{1,2}^I$ suggest that there is little asymmetry in the distribution of the interfacial dipoles. The condition $\langle R \rangle \simeq 0$ in Eq. (10) then implies symmetric $\mathcal{F}(0, R)$, which can be achieved with a reduced number of model parameters: $R_2 = -R_1$ and $F_1 = F_2 = F_0$. The free energies of the three states then become

$$\begin{aligned} F_g(R) &= R^2 / (2\kappa_g) \\ F_1(R) &= (R - R_1)^2 / (2\kappa_1) + F_0 \\ F_2(R) &= (R + R_1)^2 / (2\kappa_1) + F_0 \end{aligned} \quad (12)$$

Four model parameters κ_g , κ_1 , R_1 , and F_0 were fitted to $\sigma_R^2(m_0)$ from MD data. They are listed in Table I and are used to produce plots of $R_0(m_0)$, $\sigma_R^2(m_0)$, and $\mathcal{F}(m_0, R)$ presented in the Results section below.

TABLE I. List of model parameters produced by fitting the three-state model to $\sigma_R^2(m_0)$ from MD simulations. $\ell_R^\alpha = (\kappa_\alpha)^{-1/3}$, $\alpha = g, 1$ is the characteristic length of penetration of water's surface fluctuations into the solute [Eq. (6)].

Configuration	r_d , Å	βF_0	ℓ_R^g , Å	ℓ_R^1 , Å	R_1 , V/Å
RD9	9	7.3	3.0	3.1	0.3
RD10	10	7.2	1.5	1.2	1.0

III. RESULTS

All the simulation results that we discuss below have been produced for two distances between the point dipole in the solute and its center (Fig. 2), $r_d = 9$ Å and $r_d = 10$ Å. We will reference them throughout below as states RD9 and RD10, respectively.

There is a fairly broad intermediate region between two linear scaling regimes of the reaction field R_0 with the solute dipole m_0 . This intermediate, approximately quadratic, scaling is a signature of transitions between the low and high free energy states. This is clearly seen in the progression of free energies $\mathcal{F}(m_0, R)$ with changing m_0 shown in Fig. 5 for the RD10 state. The solid lines in the figure are obtained directly from distributions of R from MD simulations, while the dashed lines are the fits to the three-state model outlined above. The overall picture of the alteration of the free energy surface with the external dipole is remarkably consistent with the sketch shown in Fig. 1b pointing to a discontinuous, first-order character of the cross-over between the ground and excited surface states.

As is expected from the general phenomenology of discontinuous transitions,^{7,24,25} the fluctuations of the order parameter are non-Gaussian close to the transition point, reflecting transitions of the system between the two alternative states. Such enhanced fluctuations are typically reflected by spikes of variances, such as the heat capacity.²⁵ Our observations are no different and the variance $\sigma_R^2 = \langle (\delta R)^2 \rangle$ shows a peak at the transition value of the solute dipole moment (Fig. 6b). The results are plotted against a dimensionless dipole magnitude that reflects the ratio of the characteristic field produced by the solute to the one existing within the solvent

$$m_0^* = \frac{m_0}{m_s} \left(\frac{\sigma_s}{r_{ds}} \right)^3, \quad (13)$$

where m_s and σ_s are the solvent (water) dipole moment and diameter, respectively. In addition, $r_{ds} = r_{0s} - r_{HS}$ (Fig. 2) is the distance between the point dipole and the solute-water interface. Similar ideas are used to introduce the reduced instantaneous field

$$R^* = R r_{ds}^3 / m_s \quad (14)$$

the average, R_0^* , and variance, $\langle (\delta R^*)^2 \rangle$, of which are shown in Fig. 6.

The spike in the field variance is accompanied by a strong increase in the relaxation time of the

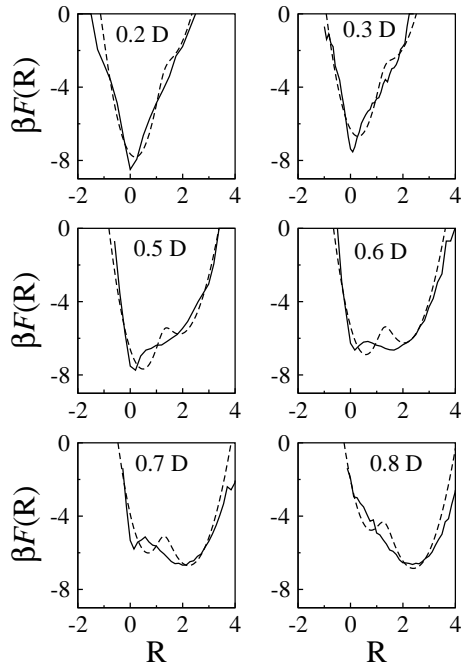


FIG. 5. Free energies $\mathcal{F}(m_0, R)$ [Eq. (3)] for the RD10 state ($r_d = 10 \text{ \AA}$) at m_0 values indicated in the plots. The reaction field in the abscissa is in V/\AA ; the dashed lines refer to the fits to the three-state model [Eqs. (8), (12)]. The model parameters used in the plot are listed in Table I.

normalized time self-correlation function, $S(t) = \langle \delta R(t) \delta R(0) \rangle / \langle (\delta R)^2 \rangle$. The relaxation time shown in Fig. 6c was calculated as $\tau_{\text{eff}} = \int_0^\infty dt S(t)$. The appearance of the peak in the relaxation time is reminiscent of critical slowing down well established for phase transitions,^{24,25} but how far that language can be carried over to our situation is not entirely clear.

The preceding discussion clearly indicates that fluctuations of water's electric field are expected to be non-Gaussian in the range of solute dipoles allowing switching of surface waters between the ground and excited states in the spirit of Figs. 1 and 5. We indeed observe a spike in the nonlinearity parameter χ_G [Eq. (4)] in the transition region (Fig. 7a). The extent and the breadth of this non-Gaussian behavior are additionally illustrated in Fig. 7b where the direct calculation of the stiffness parameter κ from the reaction field, $\kappa = R_0/m_0$, (circles) is compared to the expectation from the linear response according to Eq. (5), $\kappa = \beta \sigma_R^2$ (squares). Since the linear response function is independent of the dipole moment, the horizontal dashed line in Fig. 7b indicates the value to which both calculations would converge if linear response held. In order to provide an additional reference point to our results, the horizontal dash-dotted line shows κ for a point dipole placed inside a cavity in dielectric continuum. The reaction field in this approximation is derived

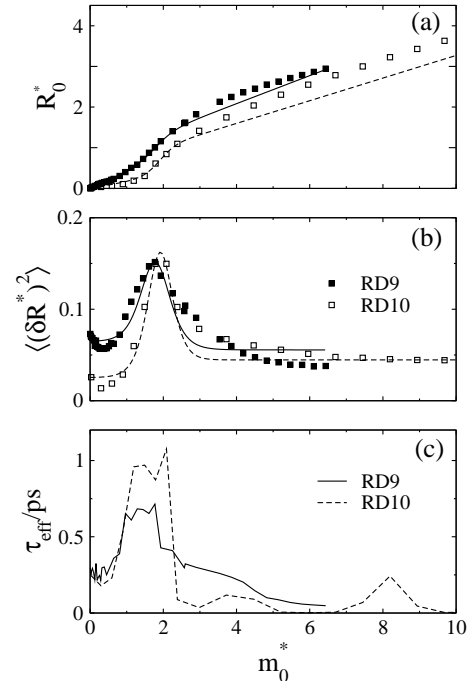


FIG. 6. The average, R_0^* , of the reduced field R^* as defined by Eq. (14) (a) and its variance (b) vs the reduced solute dipole defined by Eq. (13). The filled squares and solid lines in (a) and (b) refer, respectively, to the MD results and their fit to the three-state model for the RD9 configuration; the open squares and the dashed lines carry the same information for the RD10 configuration. Panel (c) shows the relaxation time τ_{eff} of the water field self-correlation function (see text) obtained from MD simulations for RD9 (solid line) and RD10 (dashed line) configurations.

in the SM²¹

$$R_0 = \frac{m_0}{r_{0s}^3} \frac{\epsilon - 1}{2\epsilon + 1} \left(2 - \frac{z^2}{\epsilon + 1} \right) \frac{1 + z^2}{(1 - z^2)^3}, \quad (15)$$

where $z = r_d/r_{0s}$. The continuum cavity radius in this calculation was chosen at $r_{0s} = 11.5 \text{ \AA}$, slightly below the position of the first peak of the solute-solvent pair distribution function at $\simeq 12 \text{ \AA}$ (Fig. 8).

The results presented here pose a significant question of the nature of the excited state of the surface water. A related question is what is the spatial extent of the excited water domain. The results for the alteration of the orientational order parameters with changing m_0 (Fig. 4) support the notion of a relatively localized perturbation, not spreading into the entire hydration layer.

In order to address the question of the water structure in a domain nearest to the solute dipole we have separated a solid angle of 27.4° drawn with the dipole direction as the axis and cutting a portion of the surface circumference equal to $2\sigma_s$ (see SM²¹ for a drawing). The pair solute-water distribution function was calculated for waters residing within this solid angle only and is shown in Fig. 8. A new peak emerges from the nearest solute-water distance with increasing m_0 . The area under the

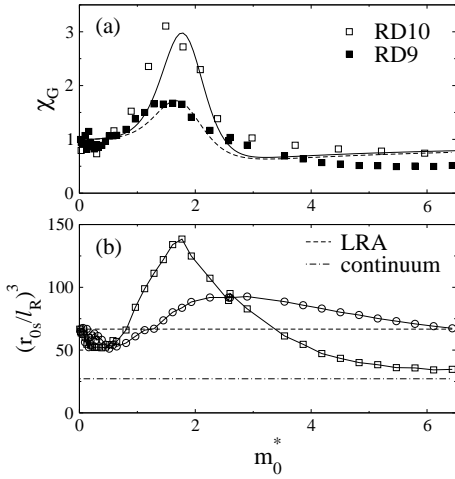


FIG. 7. Nonlinearity parameter χ_G [Eq. (4)] (a) obtained from MD simulations (points) and from fitting the three-state model (lines). Panel (b) shows the reduced stiffness parameter $\kappa r_{0s}^3 = (r_{0s}/\ell_R)^3$ calculated in different approximations for RD9. The dash-dotted line, $\kappa = R_0/m_0$, is from the dielectric continuum calculation for the reaction field at a dipole inside a dielectric cavity [Eq. (15)]. The dashed line shows $\kappa = \beta\sigma_R^2$ obtained from the variance σ_R^2 at $m_0 = 0$. The open circles show $\kappa = R_0/m_0$ and open squares refer to $\kappa = \beta\sigma_R^2$, both from MD simulations. In linear response, circles and squares are expected to collapse on the dashed line, Eq. (5).

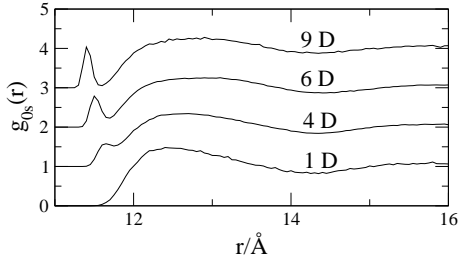


FIG. 8. Solute-oxygen pair correlation function for RD9, inside the solid angle defined in the text (see also the SM²¹). The numbers in the plot indicate values of the dipole moment m_0 . The curves are shifted vertically by 1.0 for a better view.

peak shows that exactly one water molecule breaks from the surface hydrogen-bond network, shifting toward the solute. This interpretation is consistent with the excitation free energy of $F_0 \simeq 7 k_B T$ (Table I), close to the enthalpy required to break two hydrogen bonds in SPC/E water.²⁶

The creation of the excitation defect in the hydration shell results in the frustration of the nearest bonds network seen in the alteration of the distribution of O-H-O angles of first-shell waters within the same solid angle as used in producing Fig. 8. These distributions at changing m_0 are shown in Fig. 9. Similar to the previous observations by Sharp and co-workers,¹⁸ the population of the buckled, large-angle state grows with increasing m_0 . This is a behavior generic for polar (ionic or dipolar) so-

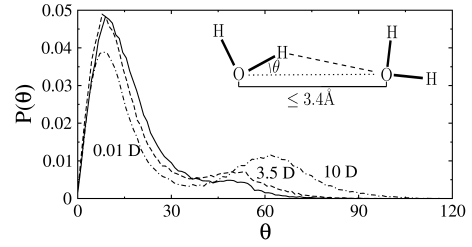


FIG. 9. Distributions of O-H-O angles θ for the RD10 configuration at m_0 equal to 0.01, 3.5, and 10 D. The distributions were calculated according to the algorithm suggested by Sharp *et al.*¹⁸ in the region of the first hydration layer within the solid angle cutting the circumference length of $2\sigma_s$ at the surface (see also the SM²¹). The inset shows the definition of the bond angle and the distance cutoff within which the angles were sampled.

lutes frustrating water's hydrogen-bond network by their electric fields.

IV. DISCUSSION

We have studied the statistics of electric field fluctuations produced by surface water inside the solute. The main finding of this study is the realization that the statistics can be profoundly altered by placing a dipole next to the interface. With increasing dipole magnitude, waters closest to the dipole alter their hydrogen-bond network in a way that creates a domain of surface waters in an excited state, with the free energy lifted by approximately the energy of breaking two hydrogen bonds ($\simeq 7 k_B T$, Table I). A crude estimate of what is needed to shift the system into this excited state is provided by Fig. 6b: a dipole twice as large as water's dipole placed one water diameter from the interface puts the system at the cross-over point at the peak of non-Gaussian fluctuations. This outcome seems to be quite generic: once surface particles have close probabilities to occupy alternative states, the variance of the fluctuations is in excess to the expectation from the linear response.²⁷

The local nature of the excitation, most likely limited to one water breaking from the network and creating a corresponding elastic deformation around it, contributes to a significant range of dipole moment magnitudes at which the system finds itself distributed between two local minima, each characterized by a linear response. This property of the local surface transition, clearly distinct from much more localized, in the parameters space, phase transitions,²⁵ will allow one to observe the effects discussed here for a substantial range of solute perturbations.

The surface defect and the corresponding frustration of the network characterizing the excitation do not necessarily require a surface dipole. They might be achieved by other causes such as ionic or hydrogen-bonding surface sites. An optical probe placed near such a domain

of waters in the excited state will record an optical response distinct in both the spectral shift and the width from probes next to the ground-state interface. In this regard, the inhomogeneous spectral broadening, which is admittedly hard to extract experimentally, is nevertheless a more sensitive probe of the local interfacial structure than the spectral shift. The Stokes shift dynamics can also slow down in the transition region, as is seen in Fig. 6c. A mosaic of ground- and excited-states domains at an extended interface of a nanometer-scale solute will then contribute to energetic and dynamic heterogeneity of the electric field fluctuations.²⁸ However, the dynamics of the electric field observed here (ps) are still significantly faster than that found for hydrated proteins (ns).^{29–31} The three orders of magnitude difference suggests a possibility of cooperativity between many surface excitations at proteins' polar/ionic surface sites. Alternatively, the excited surface state of a protein might still be localized, and the slow dynamics come as a result of protein motions modulating the interfacial polarization.³²

ACKNOWLEDGMENTS

This research was supported by the National Science Foundation (CHE-0910905). CPU time was provided by the National Science Foundation through TeraGrid resources (TG-MCB080116N).

REFERENCES

- ¹L. D. Landau and E. M. Lifshitz, *Electrodynamics of continuous media* (Pergamon, Oxford, 1984).
- ²H. Fröhlich, *Theory of dielectrics* (Oxford University Press, Oxford, 1958).
- ³C. J. F. Böttcher, *Theory of Electric Polarization*, Vol. 1 (Elsevier, Amsterdam, 1973).
- ⁴L. Onsager, *J. Am. Chem. Soc.* **58**, 1486 (1936).
- ⁵P. F. Barbara and W. Jarzaba, *Acc. Chem. Res.* **21**, 195 (1988).
- ⁶L. Reynolds, J. A. Gardecki, S. J. V. Frankland, and M. Maroncelli, *J. Phys. Chem.* **100**, 10337 (1996).
- ⁷L. D. Landau and E. M. Lifshits, *Statistical Physics* (Pergamon Press, New York, 1980).
- ⁸P. M. Chaikin and T. C. Lubensky, *Principles of condensed matter physics* (Cambridge University Press, Cambridge, 1995).
- ⁹J. P. Hansen and I. R. McDonald, *Theory of Simple Liquids* (Academic Press, Amsterdam, 2003).
- ¹⁰L. R. Pratt, G. Hummer, and A. E. Garcia, *Biophys. Chem.* **51**, 147 (1994).
- ¹¹D. V. Matyushov and M. D. Newton, *J. Phys. Chem. A* **105**, 8516 (2001).
- ¹²S. Rajamani, T. Ghosh, and S. Garde, *J. Chem. Phys.* **120**, 4457 (2004).
- ¹³D. Ben-Amotz, F. O. Raineri, and G. Stell, *J. Phys. Chem. B* **109**, 6866 (2005).
- ¹⁴A. Milischuk and D. V. Matyushov, *J. Phys. Chem. A* **106**, 2146 (2002).
- ¹⁵C. Y. Lee, J. A. McCammon, and P. J. Rossky, *J. Chem. Phys.* **80**, 4448 (1984).
- ¹⁶V. P. Sokhan and D. J. Tildesley, *Mol. Phys.* **92**, 625 (1997).
- ¹⁷P. J. Rossky, *Farad. Disc.* **146**, 13 (2010).
- ¹⁸K. A. Sharp and B. Madan, *J. Phys. Chem. B* **101**, 4343 (1997).
- ¹⁹K. A. Sharp and J. M. Vanderkooi, *Acc. Chem. Res.* **43**, 231 (2010).
- ²⁰C. Vega, E. Sanz, and J. L. F. Abascal, *J. Chem. Phys.* **122**, 114507 (2005).
- ²¹See supplementary material at [URL will be inserted by AIP] for details of the simulation protocol.
- ²²H. S. Ashbaugh, *J. Phys. Chem. B* **104**, 7235 (2000).
- ²³A. D. Friesen and D. V. Matyushov, *Chem. Phys. Lett.*, submitted(2011).
- ²⁴R. Blinc and B. Žekš, *Soft modes in ferroelectrics and antiferroelectrics* (North-Holland Publishing Co., Amsterdam, 1974).
- ²⁵K. Binder and D. W. Heermann, *Monte Carlo simulation in statistical mechanics* (Springer-Verlag, Berlin, 1992).
- ²⁶D. van der Spoel, P. J. van Maaren, P. Larsson, and N. Timneanu, *J. Phys. Chem. B* **110**, 4393 (02 2006).
- ²⁷D. V. Matyushov, *Chem. Phys.* **351**, 46 (2008).
- ²⁸N. Giovambattista, C. F. Lopez, P. J. Rossky, and P. G. Debenedetti, *Proc. Natl. Acad. Sci.* **105**, 2274 (2008).
- ²⁹P. Abbyad, X. Shi, W. Childs, T. B. McAnaney, B. E. Cohen, and S. G. Boxer, *J. Phys. Chem. B* **111**, 8269 (2007).
- ³⁰J. Tripathy and W. F. Beck, *J. Phys. Chem. B* **114**, 15958 (2010).
- ³¹D. V. Matyushov, *J. Phys. Chem. B*, submitted(2011).
- ³²B. Halle and L. Nilsson, *J. Phys. Chem. B* **113**, 8210 (2009).